Vol 14 No 4, April 2005
1009-1963/2005/14(04)/0734-10

Chinese Physics

© 2005 Chin. Phys. Soc.
and IOP Publishing Ltd

Mechanism for unidirectional movement of kinesin*

Xie Ping(谢 平), Dou Shuo-Xing(窦硕星), and Wang Peng-Ye(王鹏业)

Laboratory of Soft Matter Physics, Institute of Physics, Chinese Academy of Sciences, Beijing 100080, *China*

(Received 21 May 2004; revised manuscript received 11 August 2004)

Kinesin motors have been studied extensively both experimentally and theoretically. However, the microscopic mechanism of the processive movement of kinesin is still an open question. In this paper, we propose a hand-over-hand model for the processivity of kinesin, which is based on chemical, mechanical, and electrical couplings. In the model the ATPase rates of the two kinesin heads are regulated by forces, both from internal elasticity and external load, exerted on their necks. At a low external load, the ATPase rate of the trailing head is much higher than the leading head and the two heads are coordinated in their ATP hydrolysis and mechanical cycles. The motor walks processively with one ATP being hydrolyzed per step. At a higher forward external load, the ATPase rates of the two heads become comparable and thus the two heads are no longer well coordinated in their ATP hydrolysis and mechanical cycles. The model is consistent with the structural study of kinesin and the measured pathway of the kinesin ATPase. Using the model we have estimated the driving force to be ∼5.8pN, which is in agreement with the experimental results (5–7.5pN). The estimated time for moving one step (∼10μs) is also consistent with the measured values of 0–50μs. The previous observation of substeps within the 8nm step is explained. The shapes of velocity versus load (both positive and negative) curves show close resemblance to previous experimental results.

Keywords: kinesin, molecular motor, mechanism, dynamics
PACC: 3620, 8715B, 8715H, 8715K

1. Introduction

Conventional kinesin is a two-headed molecular motor protein that converts chemical energy of ATP hydrolysis to mechanical force. It can translocate processively and unidirectionally along a microtubule for hundreds of 8-nm steps without dissociation.[1−5] A single kinesin molecule can exert maximal forces of 5–7.5pN,[3,6−9] and at a low load its velocity can reach 800nm/s.[5,9] Conventional kinesin transports membrane-bound vesicles and organelles in various cells.[10,11]

Since its discovery, it has been studied extensively by using different experimental methods, such as biochemical, biophysical, x-ray crystallography and cryo-electron microscopy (cryo-EM); many aspects of its movement behaviour have been gradually elucidated. In particular, the rapid development and progress of single-molecule manipulation and detection techniques in recent years [12,13] have significantly improved our knowledge of its dynamic and mechanistic properties *in vitro*, with its important parameters such as stall force, velocity, mean run length, and dwell time having been determined systematically.

The microscopic mechanism of the processive movement of kinesin is still not very clear. Based on the experimental results, several models have been proposed. One is the thermal ratchet model, in which a motor is viewed as a Brownian particle moving in two (or more) periodic but spatially asymmetric stochastically switched potentials.[14,15] Another is the "hand-over-hand" model.[1,16−24] In this model, it is supposed that the motor maintains continuous attachment to the microtubule by alternately repeating single-headed and double-headed bindings. Adjacent tubulin heterodimers on the microtubule serve as the consecutive binding sites. This model requires that the two heads move in a coordinated manner and alternately move past each other. This coordination is realized by a mechanical communication between the two heads during their ATP hydrolysis cycles. The third model postulates that the kinesin head movement is coordinated through an "inchworm" mechanism,[25] in which also at least one head remains bound to the microtubule during the kinesin movement, but the two heads do not swap places, as is different from the case in the symmetric hand-over-hand model.

*Project supported by the National Natural Science Foundation of China (Grant Nos 60025516, 10334100).

For a quantitative study of the motion of kinesin, multistate chemical kinetic description is often used.[26−28] In this approach, it is postulated that the motor protein molecule steps through a sequence of discrete chemical states linked by rate constants. This approach relies mainly on biochemical observations. It can explain well some experimental results by the mechanical behaviours of kinesin, such as velocity, mean run length, and their load dependence.

In this paper, we present a hand-over-hand model that relies on chemical, mechanical, and electrical couplings. In this model, the ATPase rates of the two kinesin heads are regulated by forces exerted on their necks. Thus depending on different external loads, the two heads may or may not be coordinated in their ATP hydrolysis and mechanical cycles. At a low external load, the two heads are coordinated and the dimeric kinesin steps forward very naturally, with one ATP being hydrolyzed per step (1:1 coupling). This movement of kinesin with 1:1 coupling results essentially from the fact that the ATPase rate of the trailing head is much higher than that of the leading head at the low external load. At a higher forward external load, the two heads are no longer well coordinated in their ATP hydrolysis and mechanical cycles. Using the model we have studied the kinesin dynamics quantitatively and given good explanations to some experimental results which have not been well explained previously.

2. Structural considerations

The structural study of dimeric kinesin protein, for example, the rat brain kinesin, by using x-ray crystallography reveals that one kinesin head has +8 net elementary charges.[29] By using x-ray crystallography and cryo-EM, Kikkawa *et al*[30] revealed that each tubulin heterodimer of microtubules, i.e., the α-tubulin and β-tubulin monomers, has −27 net elementary charges (the α-tubulin monomer has −12 net charges and the β-tubulin monomer has −15 net charges). Thus, we assume that the interaction between kinesin heads and tubulin heterodimers is electrostatic. When a kinesin head is not very close to a tubulin heterodimer, the electrostatic force can be approximated as being produced by two ideal charged particles. When the kinesin head is close enough to the tubulin heterodimer, the electrostatic force is dependent on the charge distributions on the two surfaces.[31,32] So the kinesin head will bind the tubulin heterodimer in a fixed orientation.[17,33−35]

From x-ray crystallography and cyro-EM observations, it is revealed that the two kinesin heads in rigor state bind two successive tubulin heterodimers of the microtubule in equivalent orientations,[17,33,34] as schematically shown in Fig.1(a).

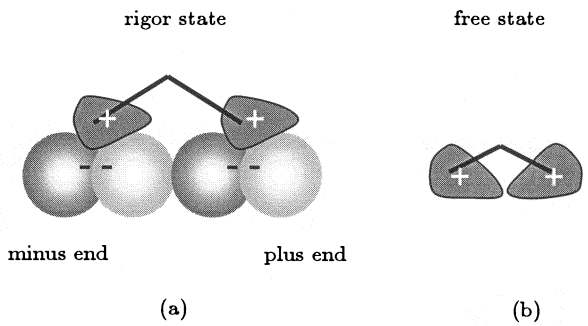


Fig.1. Schematic diagram of kinesin dimer in rigor state (a) and in free state (b). The α- and β-tubulin subunits from a single microtubule protofilament are represented by spheres in dark grey and light grey, respectively. The two kinesin heads are shown in grey. Each pair of α- and β-tubulin subunits forms a tubulin heterodimer. The polarity of the microtubule is indicated.

The determination of the crystal structure of kinesin dimer by x-ray crystallography[29] shows that its equilibrium state (or free state) corresponds to a structure as schematically shown in Fig.1(b). The two heads are related by a 120°-rotation about an axis close to that of the coiled coils (the direction of which is perpendicular to the paper surface), with an equilibrium distance (centre-of-mass distance) ∼5nm. Marx *et al*[36] further revealed that the structure of kinesin dimer in a solution is similar to the crystal structure, with the centre-of-mass distance between the two heads being slightly greater. It is taken for granted that this equilibrium state corresponds to the state that the kinesin dimer has the minimum free energy. Thus the state shown in Fig.1(a) corresponds to a state that the kinesin dimer has a greater free energy since it has a very large conformational change from its equilibrium state, both in centre-of-mass distance and relative orientation of the two heads.

Based on the principle of minimum free energy, it is anticipated that once one of the two heads or both become(s) free, the kinesin dimer structure tends to change from the state in Fig.1(a) to that in Fig.1(b). This change is realized mainly via an elastic force and an elastic torque between the two heads.

3. Model

Based on the above analysis, we propose a physical model to describe the processive and unidirectional

movement of two-headed kinesin motors along microtubules. We begin with the two kinesin heads binding to two successive tubulin heterodimers (separated by 8 nm) of the microtubules by electrostatic forces between the positively-charged heads and negatively-charged tubulin heterodimers, as shown in Fig.2(a), which is the same as Fig.1(a). In this rigor state, the structure of the kinesin dimer is highly strained. In accordance with the principle of minimum free energy, there will exist an elastic force and an elastic torque exerted on the two heads to induce the kinesin dimer changing from the state in Fig.2(a) to the equilibrium state as shown in Fig.2(b), which is the same as that in Fig.1(b), besides an electrostatic force exerted by the negatively-charged tubulin heterodimer.

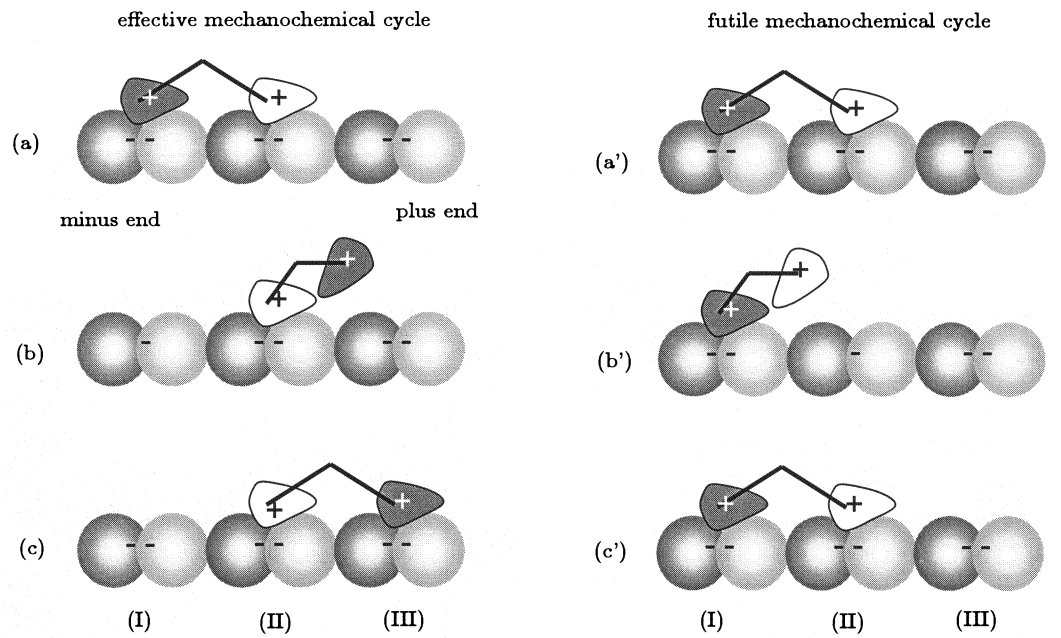


Fig.2. Schematic illustrations of kinesin movement mechanism. For clarity, the two kinesin heads are shown in grey and white. Effective mechanochemical cycle: (a) The cycle begins with both heads binding to the microtubule. (b) After ATP hydrolysis and then P_i release, the grey head (trailing head) is detached and moves towards the equilibrium position. (c) The grey head binds to the new tubulin heterodimer (III) via the electrostatic interactions and becomes the leading head for the next cycle. Futile mechanochemical cycle: (a') The cycle also begins with both heads binding to the microtubule. (b') After ATP hydrolysis and then P_i release at the white head (leading head), the white head is detached and moves towards the equilibrium position. (c') The white head rebinds to the tubulin heterodimer (II).

Activated by the microtubule, the ATPase cycles at the two heads begin. We consider two cases. (i) The ATP molecule bound to the trailing head is hydrolyzed first. The ATP hydrolysis and then P_i release lead to the weakening of the binding force,[18,20] which results from the conformational change of the kinesin head. However, the physical origin for the weakening of the binding force is still not clear. Here we make an assumption as follows. When there is the conformational change following P_i release, there appears a gap between the kinesin head and the tubulin heterodimer. Therefore, the solution will flow into the gap and certain multivalent counter-ions in the solution will bind to (or be adsorbed onto) the negatively-charged tubulin heterodimer surface, resulting in an increase of the screening effect on the negative charges of the tubulin heterodimer (for the effect of multivalent counter-ions in aqueous media on the interaction between large biological polyelectrolytes, see, for example, Ref.[37] and references therein). Then the trailing head becomes detached from the microtubule by the internal elastic force, and the kinesin dimer changes from the state in Fig.2(a) to that in Fig.2(b). In the equilibrium state of Fig.2(b), the elastic force is zero and there exists only the electrostatic force exerted by the neighbouring tubulin heterodimer (III) of the microtubule. This electrostatic force drives the detached head coming close to heterodimer (III). When close enough, the electrostatic force is dependent on the charge distributions on the two surfaces,

i.e. the interaction is sterospecific. So the head will bind the tubulin heterodimer in a fixed orientation, as shown in Fig.2(c). A forward step of 8 nm is made with one ATP being hydrolyzed (1:1 coupling) in this mechanochemical cycle. The two heads exchange their relative positions in the succeeding mechanical cycle. **(ii)** The ATP molecule bound to the leading head is hydrolyzed first. The leading head then becomes detached. Thus the kinesin dimer changes from the state in Fig.2(a') to the equilibrium state in Fig.2(b'). After the charge density of the counter-ions adsorbed onto the tubulin surface relaxes to the equilibrium (note that the charge density at the onset should be higher than that at equilibrium since, due to opposite interaction forces, the counter-ions approach the tubulin surface earlier than like-charge ions), the leading head will bind to the tubulin heterodimer (II) in the fixed orientation again by the increased electrostatic force, as shown in Fig.2(c'). One ATP is hydrolyzed in this futile mechanochemical cycle. Then the ATP molecule bound to the trailing head is hydrolyzed and the kinesin makes a forward step as in case (i). Two ATP molecules are hydrolyzed to make this forward step (2:1 coupling). After this step the ATP molecule bound to the "new" trailing head has a larger probability to be hydrolyzed earlier than that bound to the "new" leading head if the ATPase rates of the two heads are assumed to be the same.

For ATPase rates (including both ATP binding and turnover rates) of the two heads, we consider two cases. (i) The ATPase rates of the two heads are the same. In this case, the ATP molecules bound to the trailing and leading heads have equal probability to be hydrolyzed first at the beginning. Therefore, for making the first forward step there will be equal probabilities of hydrolyzing one ATP (1:1 coupling) and hydrolyzing two ATP (2:1 coupling). After the first forward step is made, there will be a higher probability of hydrolyzing one ATP molecule than of hydrolyzing two ATP per step. (ii) In the rigor state as shown in Fig.2(a), there exists a forward (i.e. the plus-end directed) force on the neck linker of the trailing head and a backward force on that of the leading head. As will be seen below, according to the energy-landscape model the ATPase rate of the trailing head will be enhanced, whereas that of the leading head will be reduced. Thus even at the beginning, the probability is high for the situation that ATP is hydrolyzed earlier at the trailing head than at the leading head. Therefore, the kinesin motor generally hydrolyzes one ATP molecule per step (1:1 coupling). As we will see in the next section, the moving time of kinesin in one step is much smaller than the ATPase time. Thus we can deduce that, in most cases, ATP hydrolysis and P_i release occur at the trailing head and ADP is released at the leading head. This is consistent with the generally-believed biochemical process.[18,20]

4. Results and discussion

4.1. Driving force

We give a simplest estimation of the magnitude of driving force for the forward movement of kinesin based on the above model. Before the equilibrium state shown in Fig.2(b) is reached, the force exerted on the trailing head is mainly an elastic force. As the equilibrium state is reached, only an electrostatic force is exerted on the free head by the neighbouring tubulin heterodimer (III). For simplicity, if we consider the tubulin heterodimer as a particle with $q_1 = -27$ charges and the kinesin head as a particle with $q_2 = +8$ charges, then the electrostatic force will be $F = \dfrac{1}{4\pi\varepsilon_r\varepsilon_0}\dfrac{q_1 q_2}{r^2}$, where the value of the relative dielectric constant for the solvent is taken to be $\varepsilon_r = 78$.[31] For simplicity, we approximate the ellipsoidal kinesin head as a sphere with radius $r_k \approx 3$nm. From Fig.3, we see that the distance between the positive charge centre of the free kinesin head and the negative charge centre of the tubulin heterodimer (III) is $r = \sqrt{[d - r_0\cos(\pi/6)]^2 + [r_0\sin(\pi/6) + d_{\text{vertical}}]^2} = 7.04$nm, where d=8nm is the distance between the two successive tubulin heterodimers, and $r_0 = 5.5$nm is the equilibrium distance between the two heads of kinesin dimer in the solution. Considering the fact that the negative charges are mainly distributed on the surfaces of the tubulin heterodimers, we take the vertical distance between the centre of the bound kinesin head and the negative charge centre of tubulin heterodimer as $d_{\text{vertical}} = 3.5$nm. Thus the electrostatic force is $F \approx 12.8$pN. Its component in the forward direction is $\sim$5.8pN, which is the driving force at this head position. This is consistent with the measured stall force of 5–7.5pN,[3,6–9] which is the force necessary to stop the motion of kinesin. Detailed discussion on stall force will be given below.

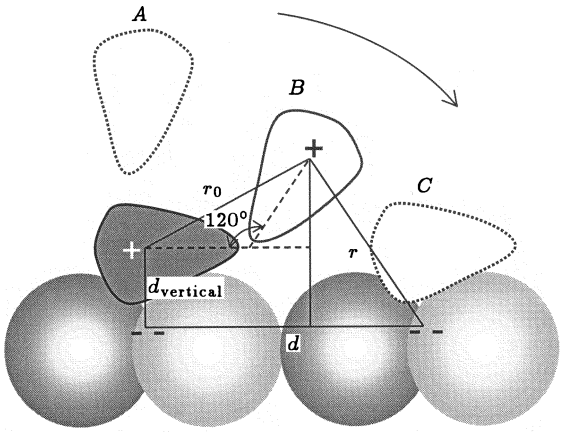


Fig.3. Geometry used to demonstrate the substeps and to calculate the distance r between the positive charge centre of the free kinesin head and the negative charge centre of tubulin heterodimer. Position A corresponds to the position that the centre of mass of the free head has the same horizontal coordinate as the bound head in grey, and position B corresponds to the equilibrium position of the free head. The line with an arrow indicates the moving direction of the free head. d is the period of the microtubule protofilament, r_0 is the free distance between the two heads of kinesin dimer in solution, and d_{vertical} is the vertical distance between the centre of the bound kinesin head and the negative charge centre of tubulin heterodimer.

4.2. Leap time

We estimate the leap time τ of the moving head, which is defined as the time for the head to move from tubulin heterodimer (I) to heterodimer (III) in Fig.2(a). To this end, we resort to the following equation for an over-damped Brownian particle:

$$\Gamma \mathrm{d}x/\mathrm{d}t = F_{\text{driving}} - F_{\text{load}} + f(t), \qquad (1)$$

where Γ is the frictional drag coefficient, $v = \mathrm{d}x/\mathrm{d}t$ is the moving velocity of the head along the microtubule, F_{driving} is the driving force on the head, and F_{load} is the force exerted on the head by the load; $f(t)$ is the fluctuating Langevin force, with $\langle f(t)\rangle = 0$ and $\langle f(t)f(t')\rangle = 2k_{\text{B}}T\Gamma\delta(t-t')$. From the Stokes formula we obtain $\Gamma = 6\pi\eta r_k = 5.65 \times 10^{-11}\text{kgs}^{-1}$, where the viscosity η of the aqueous medium of a cell around kinesin is approximately $0.01\text{gcm}^{-1}\text{s}^{-1}$. For simplicity, we approximate the driving force as a constant at any position of the moving head between tubulin heterodimers (I) and (III), which is equal to that when the head is at the equilibrium position as in Fig.2(b), i.e., $F_{\text{driving}} = 5.8\text{pN}$. In experiments the positive load is exerted on kinesin in the opposite direction of its movement with a bead connected to the two heads through a coiled-coil neck and two neck linkers. Thus it can be approximately considered that the load is always exerted on the head at leading position. So the measured rise time of the bead movement by Nishiyama *et al*[38] (or the moving time of the bead in one step) is the time for the free head to make its second half step (corresponding to positions A and C of the free head, shown in dotted lines in Fig.3), i.e. the rise time is about half of the leap time τ of the free head. When there is no load, the position of the kinesin dimer is its centre-of-mass position and thus the moving time of kinesin in one step is the leap time τ. The load is expressed as $F_{\text{load}} = F_{\text{trap}} + 6\pi\eta v r_{\text{bead}}$, where F_{trap} is the force from the optical trap and $6\pi\eta v r_{\text{bead}}$ is the Stokes force of the bead, with r_{bead} being the radius of the bead. Taking the experimental value of $r_{\text{bead}} = 0.2\mu\text{m}$ and the optical trap force $> 3\text{pN}$,[38] from Eq.(1) we obtain the rise time $5.4\mu\text{s}$ at $F_{\text{trap}} = 3\text{pN}$, $8.5\mu s$ at $F_{\text{trap}} = 4\text{pN}$, and $19\mu s$ at $F_{\text{trap}} = 5\text{pN}$. These values of rise time are consistent with the measured values of 0–50μs.[38] Note that these values of rise time are much smaller than that of the ATP turnover time, which is in the order of 10ms.[5,9,26] When there is no load, we obtain the leap time $\tau = 156\text{ns}$.

In fact, the second half-step as mentioned above is composed of two substeps. One is from position A to equilibrium position B, during which the head is mainly driven by a forward elastic force. The other is from B to C, during which the head is driven by a backward elastic force and a forward electrostatic force. As a result, the net forward driving force during the second substep may become smaller than the first substep. Thus the first substep is fast and the second substep is slow. The size of the first substep from A to B is ~4.7nm, and that of the second substep is ~3.3nm. These are qualitatively consistent with the observed substeps within the 8-nm step of single kinesin molecules.[38]

The energy required to make a forward step is $E \approx 5.8\text{pN} \times 16\text{nm} = 92.8 \times 10^{-21}\text{J}$. This is consistent with the free energy released from ATP hydrolysis ($\sim 25k_{\text{B}}T = 104 \times 10^{-21}\text{J}$).

4.3. Dynamics

We give a discussion of the moving velocity V of kinesin versus ATP concentration [ATP] and load F_{load} based on the model. As the moving time of kinesin in one step is about three orders smaller than the ATPase time, the two heads are almost always bound to the microtubule during one whole ATPase

cycle and V is actually only dependent on the ATPase rates of the two heads. The ATPase rate of each head should satisfy the Michaelis–Menten kinetics

$$K = \frac{k_c[\mathrm{ATP}]}{[\mathrm{ATP}] + k_c/k_b}, \tag{2}$$

where k_c is the ATP-turnover rate (note that the rate-limiting factors in ATP turnover are ATP hydrolysis and P_i release) and k_b is the ATP-binding rate. The dependence of the two rates, k_c and k_b, on the force, F, exerted on the head should follow the kinetics of an enzymatic reaction, which is in the general Boltzmann form.[26,39] Thus we have

$$k_c = \frac{k_c^{(0)}(1 + A_c)}{1 + A_c \exp(F\delta/k_{\mathrm{B}}T)},$$
$$k_b = \frac{k_b^{(0)}(1 + A_b)}{1 + A_b \exp(F\delta/k_{\mathrm{B}}T)}, \tag{3}$$

where $k_c^{(0)}$ ($k_b^{(0)}$) is the ATP-turnover rate (ATP-binding rate) at zero load, δ is a characteristic distance, and A is a dimensionless constant that determines the degree to which either mechanical or biochemical events limit the enzymatic reaction at vanishing load. This form of kinetic rate for an enzymatic reaction has been verified in Ref.[39] by using several classes of models. Consider here a simple model involving a sequence of sub-steps in an enzymatic reaction, with one of the sub-steps depending on force. The kinetic rate for the force-dependent sub-step, k_N, is governed by Arrhenius–Eyring kinetics, and thus it depends exponentially on the height of the energy barrier. The application of an external force, F, raises the barrier by $F\delta$ and slows the rate according to $k_N = k_N^{(0)} \exp(-F\delta/k_{\mathrm{B}}T)$.[39] Therefore, the overall time to complete an enzymatic reaction, τ, is a sum of two terms, one that is independent of force and the other that increases exponentially with force, i.e. $\tau = \tau_1 + \tau_2 \exp(F\delta/k_{\mathrm{B}}T) = (\tau_1 + \tau_2)[1+(\tau_2/\tau_1)\exp(F\delta/k_{\mathrm{B}}T)]/(1+\tau_2/\tau_1)$. The kinetic rate of the enzymatic reaction corresponds to the reciprocal of τ, which leads directly to an expression equivalent to Eq.(3).

The forces F on the neck linkers of the two heads can be written as

$$F^{\mathrm{T}} = F_{\mathrm{load}} - F_0, \tag{4a}$$

$$F^{\mathrm{L}} = F_{\mathrm{load}} + F_0, \tag{4b}$$

where F_0 is the internal elastic force, F^{T} and F^{L} are for the trailing and leading heads, respectively. Note that here we have $F_{\mathrm{load}} = F_{\mathrm{trap}}$ because the motor is in its rigor state.

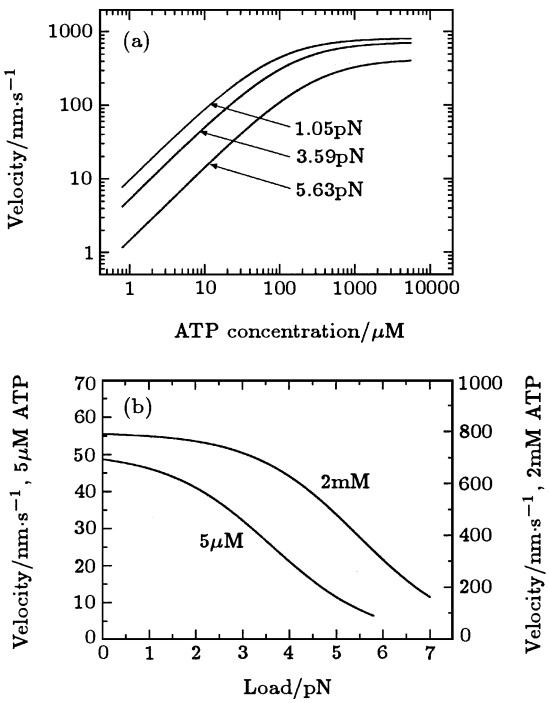


Fig.4. (a) Velocity versus [ATP] at various loads. (b) Load - velocity curves at [ATP]=5μM and [ATP]=2mM. The parameter values: δ = 3.7nm, $k_c^{(0)}$ = 49.1s^{-1}, A_c = 1.11, $k_b^{(0)}$ = 0.16μM^{-1}s^{-1}, A_b = 7.43. The elastic force between the two heads is taken as F_0 = 5.8pN.

Since for a positive load $F_{\mathrm{load}} \geq 0$ the ATPase rate of the trailing head is much faster than that of the leading head (which will be seen below), V is essentially only dependent on the ATPase rate K^{T} of the trailing head, i.e. $V = K^{\mathrm{T}} \times 8\mathrm{nm}$. Using Eqs.(2)–(4), the experimentally measured velocity of kinesin versus [ATP] and load (Figs.2 and 3a in Ref.[9]) can be fitted very well. The theoretical curves are shown in Fig.4, where the parameters are taken to be δ = 3.7nm, $k_c^{(0)}$ = 49.1s^{-1}, $k_b^{(0)}$ = 0.16μM^{-1}s^{-1}, A_c = 1.11 and A_b = 7.43, and the internal elastic force between the two heads is taken to be F_0 = 5.8pN. Using the same parameter values, we calculate the ATPase rates of the two heads for $F_{\mathrm{load}} = 0$, as shown in Fig.5. It can be seen that the ATPase rate of the trailing head is much higher than that of the leading head.

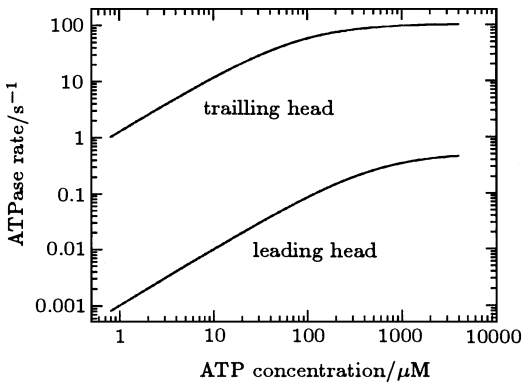


Fig.5. ATPase rates of the trailing head and leading head with no load. The parameter values are the same as in Fig.4.

When $F_{\rm load}$ becomes negative (i.e. forward load), the ATPase rate of the leading head will increase significantly and may become comparable to that of the trailing head. Thus we must consider the contributions of both heads to the kinesin movement. First, we consider that ATP binding rate of the leading head, $k_b^{\rm L}$, is not yet close to that of the trailing head, $k_b^{\rm T}$. This corresponds to the case that the load is positive or it is negative but not large enough. In this case, the probability of ATP hydrolysis of the leading head is still negligible, but that of ATP binding cannot be neglected. As the leading head becomes a new trailing head in the successive mechanical cycle, the contribution of $k_b^{\rm L}$ to the movement of kinesin is equivalent to increasing the ATP binding rate of the trailing head. The effective ATP binding rate of the trailing head can be written as (see Appendix A)

$$k_{b-\rm eff}^{\rm T} = \frac{k_b^{\rm T} + k_b^{\rm L}}{1 - k_b^{\rm L}/k_c^{\rm T}}, \qquad (5)$$

whereas the ATP turnover rate $k_{c-eff}^{\rm T}$ is still $k_c^{\rm T}$. From Eqs.(2)–(5) we can give the result of velocity V as a function of load (both positive and negative) in Fig.6. At low [ATP], ATP binding is rate limiting, and thus V is mainly determined by $k_{b-\rm eff}^{\rm T}$, which increases at most by 2-fold from 0 pN to high negative load, i.e. $k_{b-\rm eff}^{\rm T} \approx k_b^{\rm T} + k_b^{\rm L} \approx 2k_b^{\rm T}$(because $k_c^{\rm T} \gg k_b^{\rm L}$ at low [ATP]). This corresponds to the case in Figs.6(b) and (c) where the saturated V at high negative load is about two times that at 0 pN. At high [ATP], ATP turnover is rate limiting, and thus V is mainly determined by $k_c^{\rm T}$, which is already saturated when the load decreases from positive to 0 pN. Thus V increases only slightly with negative load. This corresponds to the case in Fig.6(a).

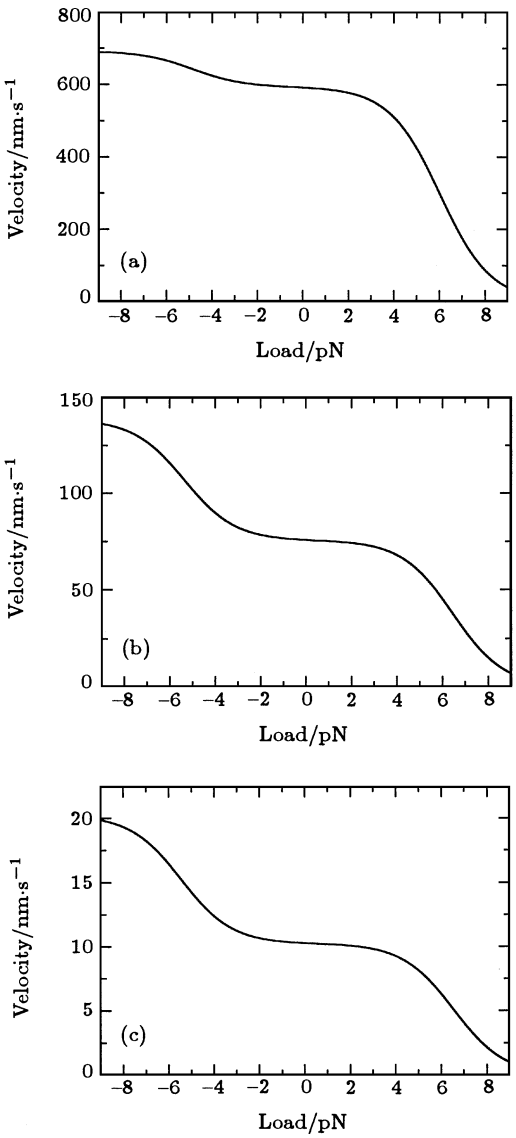


Fig.6. Load–velocity curves at (a) [ATP]=1mM, (b) [ATP] = 40μM, and (c) [ATP]=5μM. The parameter values: F_0 = 6pN, δ = 3.7nm, $k_c^{(0)}$ = 49.1s^{-1}, A_c=1.11, $k_b^{(0)}$ = 0.16μM^{-1}s^{-1}, A_b = 0.62.

The shape of the load–velocity curves in Fig.6 shows good resemblance to the experimental curves in Fig.5 of Ref.[8], especially when [ATP] is low. However, the measured V has a 3-fold increase from 0 pN to high negative load at low [ATP] (Figs.5(b) and (c) in Ref.[8]) and $\sim 50\%$ increase at high [ATP] (Fig.5(a) in Ref.[8]). We explain this discrepancy as follows. In the calculations, we have neglected the contribution of ATP hydrolysis of the leading head in the previous cycle to the ATP turnover after the leading head becomes the trailing head in the current cycle. That is, we use $k_{c-\rm eff}^{\rm T} = k_c^{\rm T}$ in the calculations. In fact, when the ATP binding rate of the leading head, $k_b^{\rm L}$, is close to that of the trailing head, $k_b^{\rm T}$, the probability is high for the ATP hydrolysis of the leading head in the pre-

vious cycle, which has begun before this head becomes the trailing head in the current cycle. This is equivalent to reducing the ATP turnover time (i.e. increasing the ATP turnover rate) of the trailing head, which results in the increase of ATPase rate K^{T} of the trailing head even at saturating [ATP]. From the experimental result at saturating [ATP] (Fig.5(a) in Ref.[8]), we may deduce that the effective ATP turnover rate $k^{\mathrm{T}}_{c-\mathrm{eff}}$ has a $\sim$50% increase at high negative load over that at no load. We expect that, at low [ATP], the ATPase rate (or V) will also have the same $\sim$50% increase due to the increase of $k^{\mathrm{T}}_{c-\mathrm{eff}}$. Therefore, due to the increases of both $k^{\mathrm{T}}_{b-\mathrm{eff}}$ and $k^{\mathrm{T}}_{c-\mathrm{eff}}$, the velocity V at low [ATP] is totally increased by $\sim$3-fold at high negative load over that at no load. For a quantitative calculation of $k^{\mathrm{T}}_{c-\mathrm{eff}}$, the probability distributions of ATP binding and turnover rates, instead of their mean values of the two heads, are required to take into consideration.

When the forward load is increased further, the probability becomes high for the ATP hydrolysis which is started and finished earlier at the leading head than at the trailing head. Thus the probability of the two ATPase cycles being coupled to one forward step for kinesin becomes high, resulting in the decrease of the moving velocity. This explains qualitatively why the moving velocity starts to drop off when the forward load is further increased in the experiment.[8] It should be noted that the observed load-velocity curves measured in Ref.[8] have not been well explained before, either qualitatively or quantitatively.

4.4. Stall force

Finally, we give an explanation of the [ATP] dependence of stall force as given in Ref.[9]. As we mentioned above, if there were no noise, the stall force would be a constant value of 5.8pN, i.e. the driving force. When noise is present, the stall force, i.e. the minimum force to stop forward movement of the free trailing head, should be equal to the driving force F_{driving} plus the "diffusion force" F_{diff} required to stop the free head diffusing $2d \approx$16nm in the forward direction. The diffusion of the free head with a force F_{diff} applied on it satisfies the equation

$$\mathrm{d}x/\mathrm{d}t = -f_{\mathrm{diff}} + \tilde{f}(t), \qquad (6)$$

where $f_{\mathrm{diff}} = F_{\mathrm{diff}}/\Gamma$; $\tilde{f}(t)$ has the property $\langle \tilde{f}(t)\rangle = 0$, $\langle \tilde{f}(t)\tilde{f}(t')\rangle = 2D\delta(t-t')$, with $D = k_{\mathrm{B}}T/\Gamma$ being the Einstein diffusion constant. From the above equation the mean first-passage time T, at which the free head diffuse a distance of $2d$, has the form (see Appendix B)

$$T = \frac{1}{f_{\mathrm{diff}}}\left[\frac{D}{f_{\mathrm{diff}}}\left(\exp\left(\frac{f_{\mathrm{diff}}}{D}2d\right)-1\right)-2d\right], \qquad (7)$$

where the mean first-passage time T should be equal to the free time of the trailing head. The free time is determined by the time for the charge density of the counter-ions adsorbed onto the tubulin heterodimer (I) surface in Fig.2(a) to decrease to the equilibrium. In calculations we take $t_{\mathrm{free}} \approx$10ms. When there are multiple ATPase cycles for the trailing head, the total free time is approximately $(K^{\mathrm{T}}t_{\mathrm{M}})t_{\mathrm{free}}$ and thus we have

$$T = K^{\mathrm{T}}t_{\mathrm{M}}t_{\mathrm{free}}, \qquad (8)$$

where $t_{\mathrm{M}} = 2$s is the time required to measure the stall force in the experiment[9] and K_{T} is the ATPase rate of the trailing head with the load F_{trap} being equal to the stall force $F_{\mathrm{stall}} = F_{\mathrm{driving}} + F_{\mathrm{diff}}$. Using the parameter values in Fig.4, $D = k_{\mathrm{B}}T/6\pi\eta r_k$, Eqs.(2)–(4), (7) and (8), we calculate F_{stall} versus [ATP]. The result is shown in Fig.7. It is seen that the theoretical curve shows similar behaviour to the experimental result (Fig.3(b) in Ref.[9]). Compared with the experimental result, the theoretical value is slightly higher. This may be due to the facts that we use the mean first-passage time instead of the first-passage time distribution and that $(K^{\mathrm{T}}t_{\mathrm{M}})t_{\mathrm{free}}$ is an overestimate of the total free time.

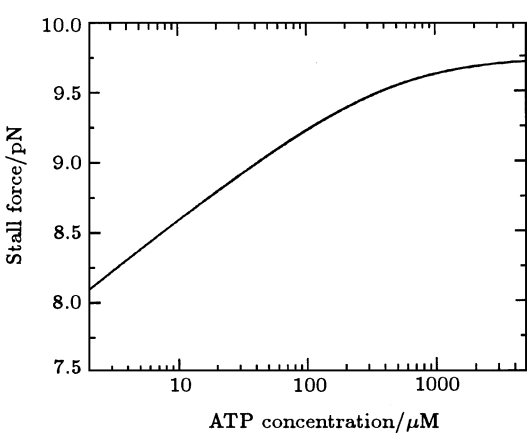


Fig.7. Stall force versus [ATP]. $F_{\mathrm{driving}} = 5.8$pN and other parameter values are the same as in Fig.4.

5. Summary

In summary, based on the previous structural and kinetic studies of dimeric kinesin motors, we present a chemically-, mechanically- and electrically-coupled model to describe the unidirectional movement of kinesin. By using the model, the estimated driving force is consistent with previous experimental results. The theoretical predictions of the moving time (i.e., rise time) in one step and existence of substeps, the velocity versus [ATP] and loads (both positive and negative), and the dependence of the stall force on [ATP] are in agreement with previous experiments.

Appendix A

We start with the moment when the trailing head just leaps forward and becomes the leading head as in Fig.2(a). Assume the dwell time of kinesin between adjacent steps is $t_{\rm dwell}$ and neglect the leap time of the trailing head in each step, then $t_{\rm dwell}$ is the time for the leading head to wait for ATP binding. It is also the ATPase time for the trailing head, thus we have

$$t_{\rm dwell} = \tau^{\rm T}_{b-{\rm eff}} + \tau^{\rm T}_c, \qquad \text{(A1)}$$

where $\tau^{\rm T}_c = 1/k^{\rm T}_c$ and $\tau^{\rm T}_{b-{\rm eff}}$ is the time taken by the trailing head for ATP binding, and thus is $\tau^{\rm T}_{b-{\rm eff}} = 1/k^{\rm T}_{b-{\rm eff}}$. As the trailing head has spent a time $t_{\rm dwell}$ in the previous cycle and thus has a ATP binding probability $k^{\rm L}_b t_{\rm dwell}$, $\tau^{\rm T}_{b-{\rm eff}}$ should satisfy

$$k^{\rm L}_b t_{\rm dwell} + k^{\rm T}_b \tau^{\rm T}_{b-{\rm eff}} = 1. \qquad \text{(A2)}$$

From Eqs.(A1) and (A2), Eq.(5) is obtained. It should be noted that Eq.(5) is only an approximation. The precise calculation of $k^{\rm T}_{b-{\rm eff}}$ needs to consider the probability distributions of ATP binding and turnover rates of the two heads.

Appendix B

From the Langevin equation, Eq.(6), we have the following Fokker–Planck equation:

$$\frac{\partial W(x,t)}{\partial t} = f_{\rm diff}\frac{\partial W(x,t)}{\partial x} + D\frac{\partial^2 W(x,t)}{\partial^2 x}.$$

Using Eq.(5.2.157) in Ref.[40], from the above equation we have

$$\begin{aligned}\psi(x) =& \exp\left[\int_a^x \left(-\frac{f_{\rm diff}}{D}\right){\rm d}x\right] \\ =& \exp\left[-\frac{f_{\rm diff}}{D}(x-a)\right],\end{aligned}$$

where the motion is supposed to be in the interval (a, b) and the barrier at a is reflecting and that at b is absorbing. In our case $2d = b - a$. Using Eq. (5.2.160) in Ref.[40], the mean first-passage time can be written as

$$T(a) = 2\int_a^b \frac{{\rm d}y}{\psi(y)}\int_a^y \frac{\psi(z)}{2D}{\rm d}z.$$

Integrating the above equation, we obtain Eq.(7).

References

[1] Howard J, Hudspeth A J and Vale R D 1989 *Nature* **342** 154

[2] Block S M, Goldstein L S and Schnapp B J 1990 *Nature* **348** 348

[3] Svoboda K, Schmidt C F, Schnapp B J and Block S M 1993 *Nature* **365** 721

[4] Schnitzer M J and Block S M 1997 *Nature* **388** 386

[5] Hua W, Young E C, Fleming M L and Gelles J 1997 *Nature* **388** 390

[6] Svoboda K and Block S M 1994 *Cell* **77** 773

[7] Meyhöfer E and Howard J 1995 *Proc. Natl. Acad. Sci. USA* **92** 574

[8] Coppin C M, Pierce D.W, Hsu L and Vale R D 1997 *Proc. Natl. Acad. Sci. USA* **94** 8539

[9] Visscher K, Schnitzer M J and Block S M 1999 *Nature* **400** 184

[10] Hirokawa N 1998 *Science* **279** 519

[11] Vale R D 2003 *Cell* **112** 467

[12] Mehta A D, Rief M, Spudich J A, Smith D A and Simmons R M 1999 *Science* **283** 1689

[13] Ishii Y, Ishijima A and Yanagida T 2001 *Trends Biotech.* **19** 211

[14] Jülicher F, Ajdari A and Prost J 1997 *Rev. Mod. Phys.* **69** 1269

[15] Astumian R D and Derenyi I 1999 *Biophys. J.* **77** 993

[16] Hackney D D 1994 *Proc. Natl. Acad. Sci. USA* **91** 6865

[17] Mandelkow E and Johnson K A 1998 *Trends Biochem. Sci.* **23** 429

[18] Gilbert S P, Moyer M L and Johnson K A 1998 *Biochemistry* **37** 792

[19] Hancock W O and Howard J 1999 *Proc. Natl. Acad. Sci. USA* **96** 13147

[20] Vale R D and Milligan R A 2000 *Science* **288** 88

[21] Fox R F and Choi M H 2001 *Phys. Rev.* E **63** 051901

[22] Asbury C L, Fehr A N and Block S M 2003 *Science* **302** 2130

[23] Yildiz A, Tomishige M, Vale R D and Selvin P R 2004 *Science* **303** 676

[24] Cross R A 2004 *Curr. Biol.* **14** R158

[25] Hua W, Chung J and Gelles J 2002 *Science* **295** 844

[26] Schnitzer M J, Visscher K and Block S M 2000 *Nat. Cell Biol.* **2** 718

[27] Keller D and Bustamante C 2000 *Biophys. J.* **78** 541

[28] Fisher M E and Kolomeisky A B 2001 *Proc. Natl. Acad. Sci. USA* **98** 7748

[29] Kozielski F, Sack S, Marx A, Thormahlen M, Schonbrunn E, Biou V, Thompson A, Mandelkow E M and Mandelkow E 1997 *Cell* **91** 985

[30] Kikkawa M, Sablin E P, Okada Y, Yajima H, Fletterick R J and Hirokawa N 2001 *Nature* **411** 439

[31] Honig B and Nicholls A 1995 *Science* **268** 1144

[32] Vale R D 1999 *Trends Cell Biol.* **9** M38

[33] Hoenger A, Sack S, Thormahlen M, Marx A, Muller J, Gross H and Mandelkow E 1998 *J. Cell Biol.* **141** 419

[34] Mandelkow E and Hoenger A 1999 *Curr. Opin. Cell Biol.* **11** 34

[35] Hirose K, Löwe J, Alonso M, Cross R A and Amos L A 1999 *Mol. Biol. Cell* **10** 2063

[36] Marx A, Thormählen M, Müller J, Sack S, Mandelkow E M and Mandelkow E 1998 *Eur. Biophys. J.* **27** 455

[37] Butler J C, Angelini T, Tang J X and Wong G C L 2003 *Phys. Rev. Lett.* **91** 028301

[38] Nishiyama M, Muto E, Inoue Y, Yanagida T and Higuchi H 2001 *Nat. Cell Biol.* **3** 425

[39] Wang M D, Schnitzer M J, Yin H, Landick R, Gelles J and Block S M 1998 *Science* **282** 902

[40] Gardiner C W 1983 *Handbook of Stochastic Methods for Physics, Chemistry and the Natural Sciences* (Berlin: Springer)